



HAL
open science

Interest of phenomic prediction as an alternative to genomic prediction in grapevine

Charlotte Brault, Juliette Lazerges, Agnes Doligez, Miguel Thomas, Martin Ecartot, Pierre Roumet, Yves Bertrand, Gilles Berger, Thierry Pons, Pierre François, et al.

► To cite this version:

Charlotte Brault, Juliette Lazerges, Agnes Doligez, Miguel Thomas, Martin Ecartot, et al.. Interest of phenomic prediction as an alternative to genomic prediction in grapevine. *Plant Methods*, 2022, 18, 10.1186/s13007-022-00940-9 . hal-03884933

HAL Id: hal-03884933

<https://hal.science/hal-03884933>

Submitted on 5 Dec 2022

HAL is a multi-disciplinary open access archive for the deposit and dissemination of scientific research documents, whether they are published or not. The documents may come from teaching and research institutions in France or abroad, or from public or private research centers.

L'archive ouverte pluridisciplinaire **HAL**, est destinée au dépôt et à la diffusion de documents scientifiques de niveau recherche, publiés ou non, émanant des établissements d'enseignement et de recherche français ou étrangers, des laboratoires publics ou privés.

RESEARCH

Open Access



Interest of phenomic prediction as an alternative to genomic prediction in grapevine

Charlotte Brault^{1,2,3}, Juliette Lazerges^{1,2}, Agnès Doligez^{1,2}, Miguel Thomas^{1,2}, Martin Ecarnot¹, Pierre Roumet¹, Yves Bertrand^{1,2}, Gilles Berger^{1,2}, Thierry Pons^{1,2}, Pierre François^{1,2}, Loïc Le Cunff^{1,2,3}, Patrice This^{1,2} and Vincent Segura^{1,2*}

Abstract

Background: Phenomic prediction has been defined as an alternative to genomic prediction by using spectra instead of molecular markers. A reflectance spectrum provides information on the biochemical composition within a tissue, itself being under genetic determinism. Thus, a relationship matrix built from spectra could potentially capture genetic signal. This new methodology has been mainly applied in several annual crop species but little is known so far about its interest in perennial species. Besides, phenomic prediction has only been tested for a restricted set of traits, mainly related to yield or phenology. This study aims at applying phenomic prediction for the first time in grapevine, using spectra collected on two tissues and over two consecutive years, on two populations and for 15 traits, related to berry composition, phenology, morphological and vigour. A major novelty of this study was to collect spectra and phenotypes several years apart from each other. First, we characterized the genetic signal in spectra and under which condition it could be maximized, then phenomic predictive ability was compared to genomic predictive ability.

Results: For the first time, we showed that the similarity between spectra and genomic relationship matrices was stable across tissues or years, but variable across populations, with co-inertia around 0.3 and 0.6 for diversity panel and half-diallel populations, respectively. Applying a mixed model on spectra data increased phenomic predictive ability, while using spectra collected on wood or leaves from one year or another had less impact. Differences between populations were also observed for predictive ability of phenomic prediction, with an average of 0.27 for the diversity panel and 0.35 for the half-diallel. For both populations, a significant positive correlation was found across traits between predictive ability of genomic and phenomic predictions.

Conclusion: NIRS is a new low-cost alternative to genotyping for predicting complex traits in perennial species such as grapevine. Having spectra and phenotypes from different years allowed us to exclude genotype-by-environment interactions and confirms that phenomic prediction can rely only on genetics.

Keywords: Phenomic prediction, Genomic prediction, Plant breeding, Spectroscopy, Phenomics, Grapevine

Background

Viticulture has to face two major threats in the next decades, diseases and climate change, which impact both yield and wine quality. Plant breeding could help mitigating these impacts by mobilizing grapevine genetic diversity [21]. However, grapevine breeding is slow because

*Correspondence: vincent.segura@inrae.fr

¹ UMR AGAP Institut, Univ Montpellier, CIRAD, INRAE, Institut Agro Montpellier, Montpellier 34398, France
Full list of author information is available at the end of the article



© The Author(s) 2022. **Open Access** This article is licensed under a Creative Commons Attribution 4.0 International License, which permits use, sharing, adaptation, distribution and reproduction in any medium or format, as long as you give appropriate credit to the original author(s) and the source, provide a link to the Creative Commons licence, and indicate if changes were made. The images or other third party material in this article are included in the article's Creative Commons licence, unless indicated otherwise in a credit line to the material. If material is not included in the article's Creative Commons licence and your intended use is not permitted by statutory regulation or exceeds the permitted use, you will need to obtain permission directly from the copyright holder. To view a copy of this licence, visit <http://creativecommons.org/licenses/by/4.0/>. The Creative Commons Public Domain Dedication waiver (<http://creativecommons.org/publicdomain/zero/1.0/>) applies to the data made available in this article, unless otherwise stated in a credit line to the data.

of the long juvenile period and cumbersomeness of field trials. Indeed, phenotyping requires 6 to 7 years in grapevine, and breeding cycles traditionally last at least 15 years. Genomic prediction (GP), first proposed by Bernardo et al. [2] and Meuwissen et al. [18] is a promising tool to speed up breeding programs and increase selection accuracy, by using genomic information to predict breeding values of candidates to selection. Even though genotyping costs have decreased drastically during the last decades, they can still be prohibitive when hundreds of selection candidates have to be genotyped. That is why Rincent et al. [24] proposed to switch from genomic markers to near-infrared spectra (NIRS) measured on plant tissues, in a new concept called phenomic prediction (PP). The relationship matrix based on NIRS is indeed expected to share similarities with the genomic relationship matrix, because a reflectance spectrum is determined by the biochemical composition of the analyzed sample (Beer-Lambert law), which in turn is determined by genetic and environmental factors. As PP uses endophenotypes such as NIRS, it may better account for non-additive genetic effects. In addition, besides being cheaper, NIR measurements are high-throughput, which is required for screening the large populations typically evaluated in breeding programs. One step further, Robert et al. [26] proposed a definition of genomic-like omics based (GLOB) prediction, which encompasses both phenomic and other omics-based prediction as in Schrag et al. [28]. GLOB is a particular configuration where NIRS (or other omics) used for model training and prediction come from different environments.

Rincent et al. [24] found that phenomic predictive ability could be higher than genomic predictive ability with wheat grain NIRS and equivalent predictive ability (PA) with poplar wood NIRS for some traits. In wheat, when predicting across environments, PP was still more accurate than GP for most traits.

Other studies, such as Lane et al. [16] in maize reported PA for PP, but in this study, GP was not implemented for comparison. Krause et al. [15] applied PP in wheat in a single environment with hyperspectral imaging from different phenological stages, they found higher PA with PP than with GP for most time-points studied. Indeed, this might be explained thanks to genotype-by-environment ($G \times E$) interactions, because NIRS on training set (TS) and validation set (VS) were measured in a single environment, and spectra and traits were collected the same years. Several studies also reported an increase in PA when combining genomic and phenomic matrices in a single prediction model [6, 12]. Nevertheless, PP is still in its infancy, as it has been mostly applied to cereals with grain and leaves as tissues. Many issues remain, in particular which could be the best way to implement PP in

breeding programs. In the case of perennial species, such as grapevine, year effect is known to strongly affect phenotype, and how behaves PP in this context remains to be studied. Also, in the case of woody perennial, wood matter offers another kind of material for collecting spectra which could be complementary to leaves. Rincent et al. [24] found in wheat that combining NIRS collected on leaves and grains could enhance the PA for some cases. More work is thus required to devise a strategy for implementing PP in breeding programs.

In grapevine, GS has been already implemented and gave promising results on different populations [3, 4, 9, 10]. However, so far to our knowledge only one study has evaluated PP in woody perennials (in poplar [24]) and consequently none on grapevine.

The aim of this study was to understand under which configuration PP could be implemented in grapevine breeding programs. For that, we used spectra and phenotypes collected different years apart, in order to minimize $G \times E$ interaction effects, which are typically captured by spectra. It allows us to disconnect phenomic prediction from $G \times E$. We first provided a thorough characterization of the genetic signal in spectra. Specifically, we performed a co-inertia analysis [7] to assess the covariation between genotyping and NIRS matrices. This methodology was already used in ecology and multi-omics studies but has never been applied in this context [17, 19]. It consists in maximizing the covariance between eigenvectors of matrices. By using co-inertia analysis, we wanted to assess to what extent spectra provide similar information as molecular markers, in terms of genetic relationship.

Then, we compared multiple configurations for performing PP, such as using raw NIRS vs. derived BLUPs over a single or two years and over a single or two tissues. Finally, three distinct questions were answered: what is the best configuration for performing PP? How do phenomic PA performs compared to genomic PA? Can adding NIRS to genotypic data increase PA?

Material and methods

Plant material

Our plant material is composed of a diversity panel reflecting the whole genetic diversity of *Vitis vinifera* [22] and a half-diallel [29], more similar to the populations used in breeding programs.

The diversity panel is composed of 279 varieties, with an equal proportion of individuals from each of the three gene pools: Wine West (WW), Wine East (WE) and Table East (TE) [22]. This panel was overgrafted on Marselan in 2009, itself grafted on Fercal. Field location is in the Domaine du Chapitre experimental vineyard of Institut Agro | Montpellier SupAgro in Villeneuve-lès-Maguelone

(South of France). The panel is replicated in five randomized complete blocks, each variety being represented by one plot of a single vine in each block.

The half-diallel is composed of 676 individuals from ten bi-parental populations (hereafter named crosses) in a half-diallel mating design between five parents: Syrah (S), Grenache (G), Cabernet-Sauvignon (CS), Terret Noir (TN) and Pinot Noir (PN) [29]. All of them, except Grenache, belong to the WW gene pool [4]. Each cross comprises between 64 and 70 offspring. This population was planted in 2005 and grafted on Richter 110. Field location is the same experimental vineyard, a few kilometers away from the diversity panel field trial. The half-diallel is replicated in two randomized complete blocks, each offspring being represented by one plot of two consecutive vines in each block.

Phenotyping

We studied the same 15 traits in both trials (diversity panel and half-diallel). Phenotypic data were collected in 2011 and 2012 for the diversity panel and between 2013 and 2017 for the half-diallel. Traits were related to (i) berry composition at harvest, with malic acid (**mal.ripe**), tartaric acid (**tar.ripe**), shikimic acid (**shik.ripe**) concentrations, and shikimic to tartaric acid (**shiktar.ripe**) and malic to tartaric acid (**maltar.ripe**) ratios, (ii) berry and cluster morphological traits, with mean berry weight (**mbw**), mean cluster weight (**mcw**), mean cluster length (**mcl**), mean cluster width (**mcwi**) and cluster compactness (**clucomp**), (iii) phenology traits, with véraison date (onset of ripening, **verday**), harvest date (**samplday**) and the interval between véraison and harvest (**vermatu**), (iv) vigor (**vigour**). Details about phenotypic measurements, statistical processing and heritability can be found in Brault et al. [4]. For prediction, we used the Best Linear Unbiased Predictors (BLUP) of genotypic values from Flutre et al. [9] in the diversity panel and Brault et al. [4] in the half-diallel. Briefly, a mixed linear model was fitted for eliminating experimental confounding effects and in order to extract BLUPs of genotypic values. In the following, only BLUPs of genotypic values were used for the diversity panel, whereas the sum of genotypic and cross BLUPs were used for the half-diallel.

SNP genotyping

We used a set of 32,894 SNP markers common to both populations, coming from genotyping-by-sequencing technology (*ApeKI*) [8], using Illumina Hi-seq sequencing. Details about genotyping and marker processing are given in Tello et al. [29] for the half-diallel and in Flutre et al. [9] for the diversity panel. The selection of common SNPs was done in Brault [4]. 622 out of 676 individuals

were successfully genotyped in the half-diallel, and 277 out of 279 individuals in the diversity panel.

Spectra measurements

Spectra were measured in both trials on dried wood and leaves collected during two consecutive years (2020 and 2021). For wood tissue, two shoots were cut per plot, on two vines in the half-diallel and one in the diversity panel. These wood shoots were approximately 3 cm long. Wood was harvested on January 27th in 2020 and January 14th in 2021. For leaf tissue, four discs were sampled per plot, on two adult leaves per vine for two different vines in the half-diallel and on four leaves per vine in the diversity panel. Leaf disks had diameters of *circa* 1 cm and 0.5 cm in 2020 and 2021, respectively. Leaf tissue harvest occurred on July 1st 2020 and June 16th 2021. Two blocks were used in both trials, leading to a total of four wood shoots and eight leaf discs per genotype. After harvest, shoots and leaves were dried at 60°C until the weight stopped decreasing, and then stored in a cold chamber until measurements. For each tissue, spectra measurements for both populations lasted a few weeks.

For spectra gathering, a reflectance probe plugged to a visible-infrared spectrometer was used (LabSpec 2500 Portable Vis/Nir spectrometer device ; Analytical Spectral Devices, Inc., Boulder, CO, US) with its associated software IndicoPro 6.5. A reference spectrum was taken twice a day, using Spectralon[®]. For each wood shoot, two scans were taken, one on each end of the shoot. For each leaf disc, one scan was taken, on the adaxial surface. Thus, for each tissue, four scans were produced per plot (i.e., per genotype × block combination). Wavelengths ranged from 350 to 2,500 nm, with a 1 nm step. For each scan, the spectrometer takes 10 spectra which are automatically averaged to make one spectrum record. In total around 1800 and 5400 scans were collected on the diversity panel and the half-diallel populations for each year and tissue, respectively.

Spectra pre-processing

Spectra were processed separately within each trial. The first 50 wavelengths (visible range) were cut, because of instabilities. The average of the four spectra per plot were then carried out over the 2101 remaining wavelengths. From these averaged raw spectra (**raw**), five pre-processing were then applied: smoothing (**smooth**) using Savitzky-Golay [27] procedure, normalization or standard normal variate (**snv**) which consists in centering and scaling [1], detrend (**dt**) for removing baseline [1], and first and second derivative on normalized spectra (**der1** and **der2**, respectively), also for removing baseline and exacerbate some parts of the signal.

Table 1 Mixed model fitted, depending on the model combination

	Wood	Leaves	Wood + leaves
2020	1	1	1 + <u>geno : tissue</u> + <u>cross : tissue</u>
2021	1	1	1 + <u>geno : tissue</u> + <u>cross : tissue</u>
2020 + 2021	1 + <u>geno : year</u> + <u>cross : year</u>	1 + <u>geno : year</u> + <u>cross : year</u>	1 + <u>geno : tissue</u> + <u>cross : tissue</u> + <u>geno : year</u> + <u>cross : year</u>

cross effect is replaced by *subpop* for the diversity panel. 1 corresponds to the mixed model specified in Eq. 1

On each of these six spectra matrices (**raw**, **smooth**, **snv**, **dt**, **der1** and **der2**), we applied a mixed model over the reflectance at each wavelength, to compute variance components and derive NIRS genotypic BLUPs for each possible combination of three models at the tissue level times three models at the year level (Table 1).

The mixed model was:

$$r_{ijk} = \mu + \text{geno}_i + \text{cross/subpop}_i + \text{block}_j + \underline{x} + \underline{y} + \epsilon_{ijk} \tag{1}$$

With *r* the reflectance at a given wavelength, μ the intercept, *geno* the random genotypic effect, *cross/subpop* the random effect for cross (10 levels in the half-diallel) or subpopulation (3 levels in the diversity panel) effect, *block* the fixed effect of block, *x* and *y* the random effects for plot coordinates, and ϵ the residuals.

Factors could then be added to this base model, depending on the model combination (Table 1).

NIRS BLUPs used further were the sum of genotypic and cross or subpopulation BLUPs. For comparison, we also computed genotypic BLUPs from models without *cross* or *subpopulation* effects.

For comparison purpose and to evaluate the benefit of fitting a mixed model per wavelength to extract a genotypic BLUP (i.e. BLUP spectra), we also computed for each of the 6 spectra matrices (**raw**, **smooth**, **snv**, **dt**, **der1** and **der2**) the averaged spectra per genotype, this configuration was called *base* spectra.

Variance components and co-inertia

Variance components from mixed models were extracted at each wavelength and compared between model combinations and populations.

We also compared relationship matrices obtained independently from SNPs (that is, the genomic relationship matrix) and NIRS BLUPs (that could be called the phenomic relationship matrix), using co-inertia analysis [7]. Briefly, the co-inertia between two matrices X and Y (from SNP and wood NIRS for example) is computed as:

$\text{coinertia}(X, Y) = \text{trace}(XQ_X X^T D Y Q_Y Y^T D)$, with Q_X and Q_Y the weights associated with X and Y columns (SNP markers and reflectances), which were set to 1, and

D the weights associated with X and Y rows (individuals), which were set to 1/n with n the number of individuals.

Then, a measure of correlation between X and Y can be computed as the RV coefficient [25]:

$$RV = \frac{\text{coinertia}(X, Y)}{\sqrt{\text{coinertia}(X, X)} \sqrt{\text{coinertia}(Y, Y)}}$$

We applied co-inertia analysis to SNPs, wood and leaf NIRS BLUPs, in order to estimate pairwise RV coefficients between these matrices.

Heritability assessment

Heritability values of phenotypic data were assessed for both populations in Flutre et al. [9] for the diversity panel and in Brault et al. [4] for the half-diallel. Broad-sense heritability values ranged between 0.53 and 0.91 for the half-diallel and between 0.72 and 0.97 for the diversity panel.

Heritability values were also assessed for reflectance data at each wavelength, after mixed model fitting. As for phenotypic data, heritability formula was calculated on an entry-mean basis, as described in Piepho et al. [23]:

$$H^2 = \frac{\sigma_{\text{geno}}^2 + \sigma_{\text{cross}}^2}{\sigma_{\text{geno}}^2 + \sigma_{\text{cross}}^2 + \frac{\sigma_{\text{geno:year}}^2 + \sigma_{\text{cross:year}}^2}{n_{\text{year}}} + \frac{\sigma_x^2 + \sigma_y^2 + \sigma_\epsilon^2}{n_{\text{rep}} \times n_{\text{year}}}}$$

with the variance components previously estimated in the mixed model, $n_{\text{rep,year}}$ the mean number of replicates per year, and n_{year} the number of year (one or two, depending on the model).

Phenomic and genomic prediction models

Three methods were compared for the implementation of PP and GP, based on two models. Models were fitted separately for each population and trait.

rrBLUP vs GBLUP model type

- In rrBLUP, we fitted the following model: $y = X\beta + \epsilon$, with *y* the vector of genotypic BLUPs from phenotypic data, *X* the matrix for marker genotypes (additively coded as in Brault et al. [4]) or wavelength data (from NIRS BLUPs for each of the nine above-mentioned model combinations), β the marker or wavelength effects and ϵ the residual effects. This model was fitted using R/glmnet package version

4.1-2 [11]. In rrBLUP, marker or wavelength effects are shrunk towards zero, according to a regularization parameter, chosen by an inner cross-validation (CV).

- In GBLUP model (using the NIRS or the genomic relationship matrix), we fitted the following model: $y = u + \epsilon$, with y the vector of genotypic BLUPs from phenotypic data, u the random effects for genomic or phenomic estimated breeding value, with $u \sim \mathcal{N}(0, \sigma_u^2 K)$, K being the relationship matrix from markers or spectra, σ_u^2 the genetic variance, and ϵ the random residual effect, $\epsilon \sim \mathcal{N}(0, \sigma_\epsilon^2 I)$, I being the identity matrix. $K = \frac{X_{sc} X_{sc}^T}{nb \text{ of } X_{sc} \text{ columns}}$, X_{sc} the previously described X matrix scaled on allelic frequencies or wavelength reflectances. This model was fitted using R/lme4GS package version 0.1 [5].

Multi-matrix model fitting

Using R/lme4GS allowed us to fit a single model involving several variance-covariance matrices, such as: $y = \sum_{j=1}^q u_j + \epsilon$, with $u_j \sim \mathcal{N}(0, \sigma_j^2 K_j)$, and K_j the relationship matrix from SNPs, wood NIRS or leaf NIRS previously described. We fitted this multi-matrix model using two or three variance-covariance matrices: SNPs + wood NIRS, SNPs + leaf NIRS, wood NIRS + leaf NIRS and SNPs + wood NIRS + leaf NIRS.

Cross-validation

PP and GP models were assessed within each population and for each trait using CV. In order to equalize the TS size between populations, a 10-fold CV was applied in the half-diallel, while a 5-fold CV was applied in the diversity panel. CV was repeated 10 times. For each CV replicate, predicted values from all folds were combined and compared with observed genotypic BLUPs. We computed predictive ability (PA) as Pearson’s correlation between the observed and predicted genotypic values. In the half-diallel, PA was calculated within each cross, as it was done in Brault et al. [4]. Predicted genotypic values were separated per cross and predictive ability was calculated for each of the ten crosses.

Results

Characterization of genetic signal in spectra

Variance components

Variance components for the nine model combinations studied in each population are shown in Fig. 1 for **der1** pre-processing, the pre-process with the highest heritability (Additional file 1: Fig. S1). In both populations,

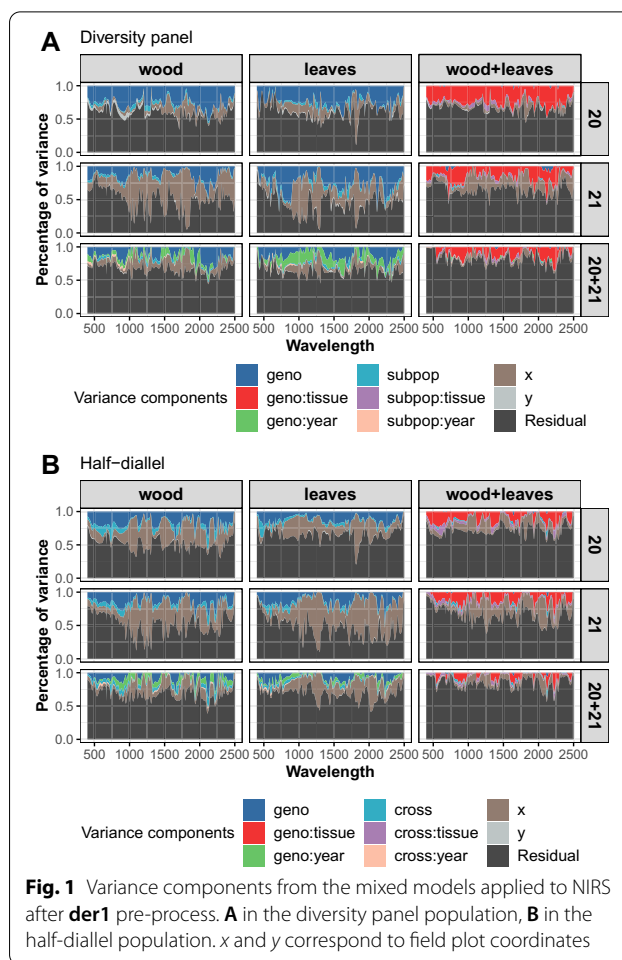
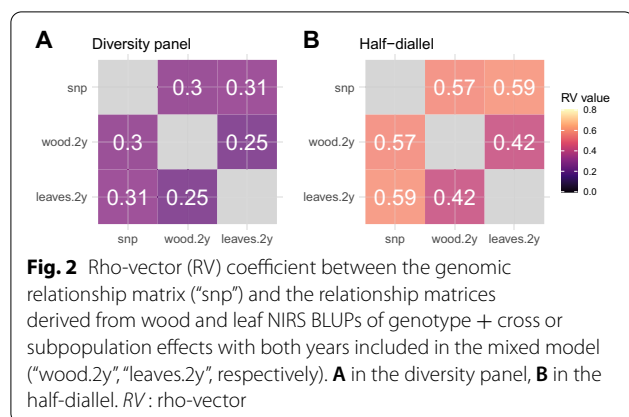


Fig. 1 Variance components from the mixed models applied to NIRS after **der1** pre-process. **A** in the diversity panel population, **B** in the half-diallel population. x and y correspond to field plot coordinates

genotypic variance was maximized in single-year and single-tissue analyses. The genotypic variance had the same magnitude between years (2020 and 2021) and between tissues (leaf and wood). In multi-tissue analyses, genotypic variance drastically decreased and was mostly replaced by the *geno:tissue* interaction variance, while in multi-year analyses, genotypic variance was only partly replaced by the *geno:year* interaction variance. A strong x effect (row effect) was observed, while barely no y effect was present.

Comparing populations, the *cross* variance in the half-diallel was larger than the *subpop* variance in the diversity panel. The variance of interactions between *cross* or *subpop* and *year* or *tissue* remained low. The *geno:year* interaction was more important in the diversity panel than in the half-diallel for leaf tissue, and comparable for wood tissue.



Heritability

Genotypic variance results were consistent with heritability values calculated for each wavelength (distributions of heritability values for each pre-process are given in Additional file 1: Fig. S1).

When comparing raw and pre-processed spectra, it was clear that the lowest heritability values generally corresponded to **raw** and **smooth** spectra. Heritability values for other pre-processes were close to each other, **der1** yielding the highest heritability values overall (Additional file 1: Fig. S1).

Including both wood and leaf NIRS in the mixed model resulted in very low heritability values (Additional file 1: Fig. S2), hence we excluded this model in the following analyses. The analysis wavelength by wavelength has showed that NIRS carry some genetic variance, with a moderate magnitude. To further characterize this genetic signal over the entire spectral range, we then carried out a co-inertia analysis between NIRS and SNP matrices.

Comparison of matrices from SNPs and NIRS, using co-inertia analysis

Co-inertia analysis was conducted on single-tissue models only. Figure 2 shows for each population the relative co-inertia between three matrices of SNPs, wood and leaf NIRS BLUPs of *genotype* + *cross* or subpopulation effects for "2 years" models. For both populations, correlation with SNPs was similar between wood and leaf NIRS. However, this correlation was nearly twice higher in the half-diallel than in the diversity panel. It is noteworthy that in both populations the correlation between the SNP matrix and NIRS BLUPs matrices (obtained from wood or leaves) was higher than between the two NIRS BLUPs matrices obtained on wood and leaves.

We also carried out the co-inertia analysis with matrices derived from NIRS BLUPs of *genotype* effect for a model containing either a *genotype* effect only or both

genotype and *cross* or *subpopulation* effects (Additional file 1: Fig. S2).

Using such matrices strongly decreased correlation with the SNP matrix, as compared to using matrices derived from BLUPs of *genotype* + *cross* or *subpopulation* effects (Additional file 1: Fig. S2). Therefore, in subsequent prediction analyses, we used only the latter matrices including *cross* or *subpopulation* effect. Matrices from multi-year NIRS BLUPs generally displayed a slightly higher correlation with the SNP matrix than the single-year BLUPs, and this effect was more pronounced in the half-diallel (Additional file 1: Fig. S3).

Phenomic prediction using BLUPs vs base spectra and rrBLUP vs GBLUP

In each population and across both tissues and both years, using spectra BLUPs instead of *base* spectra almost always resulted in higher PA (Fig. 3). However, differences were observed depending on the method and population. The method yielding the highest PA was GBLUP (implemented with lme4GS) in the half-diallel and rrBLUP (implemented with glmnet) in the diversity panel. However, it is worth mentioning that differences between methods were found to be more pronounced in the half-diallel than in the diversity panel. The highest differences between *base* spectra and BLUPs were observed for the best method in each population.

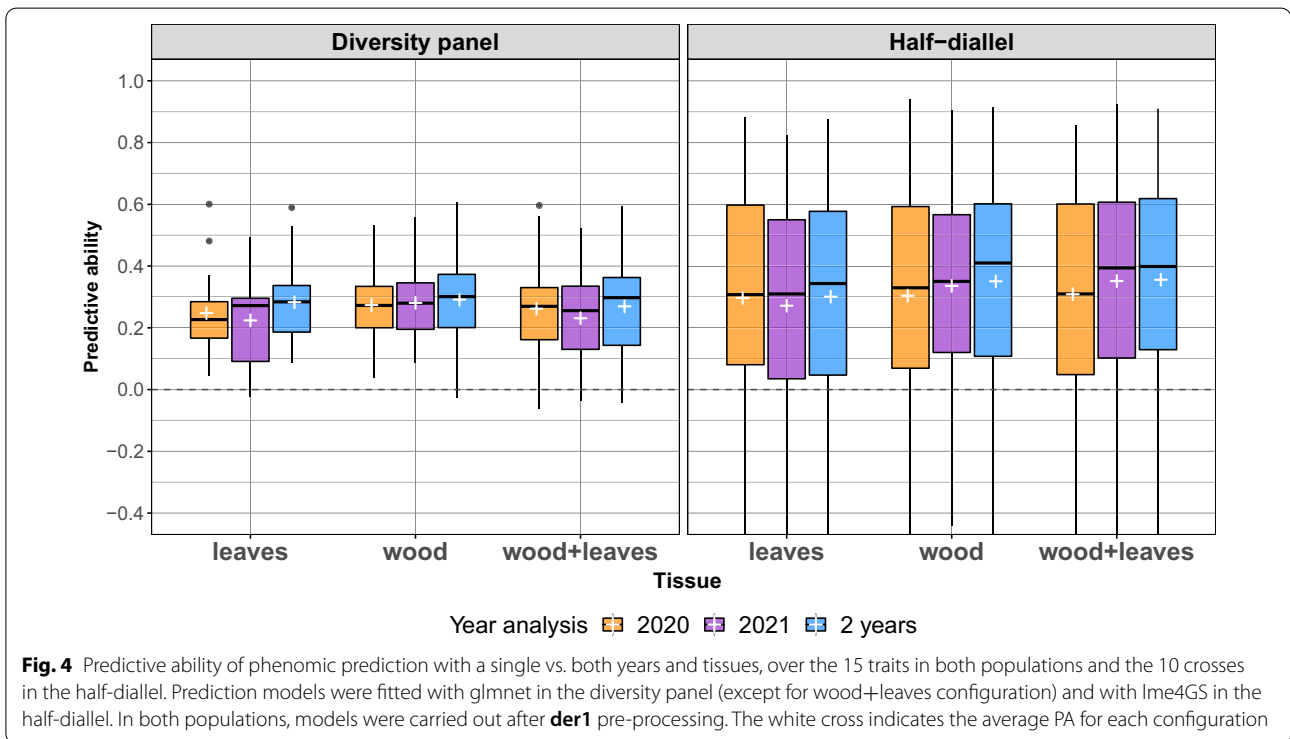
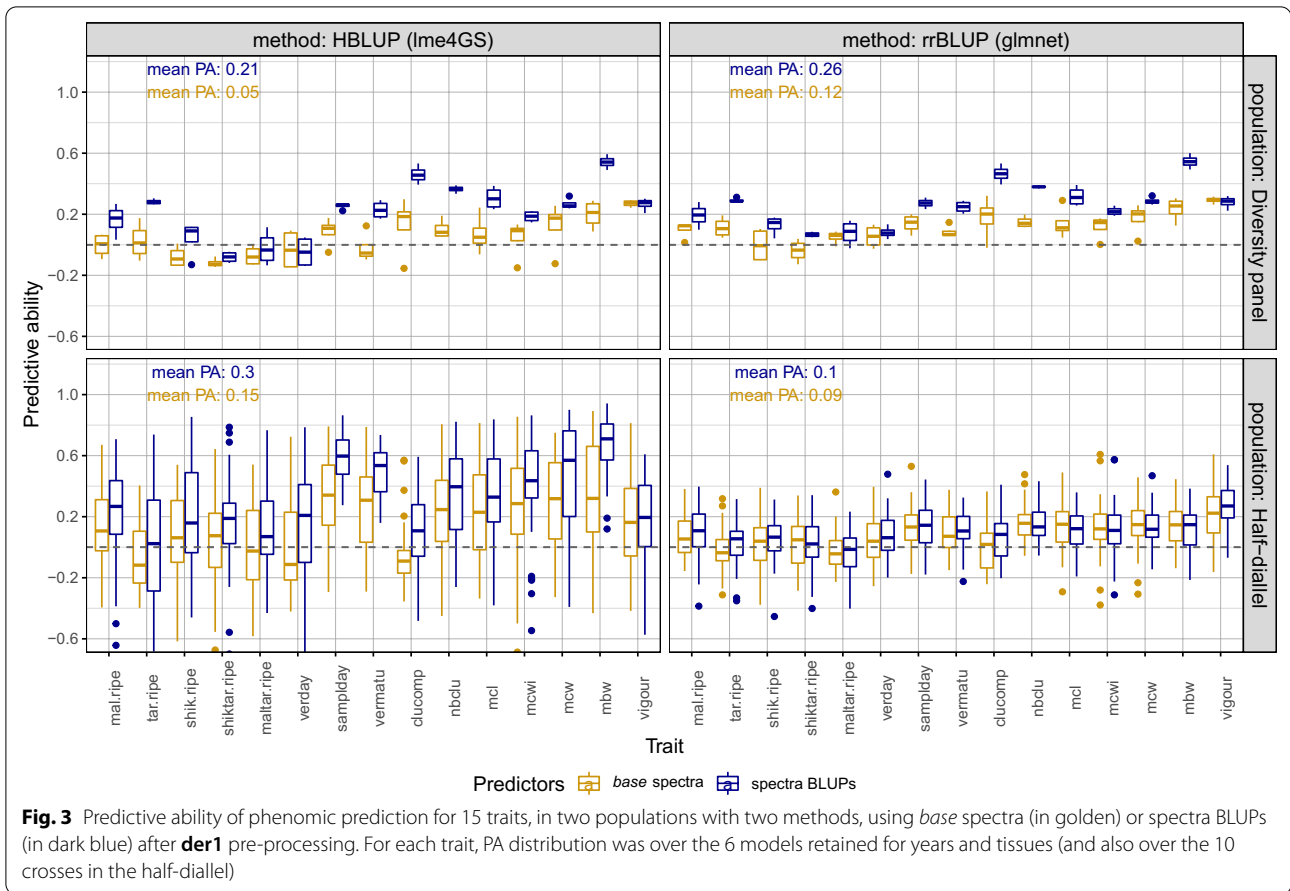
Thus, we retained spectra BLUPs in all cases, lme4GS in the half-diallel and glmnet in the diversity panel.

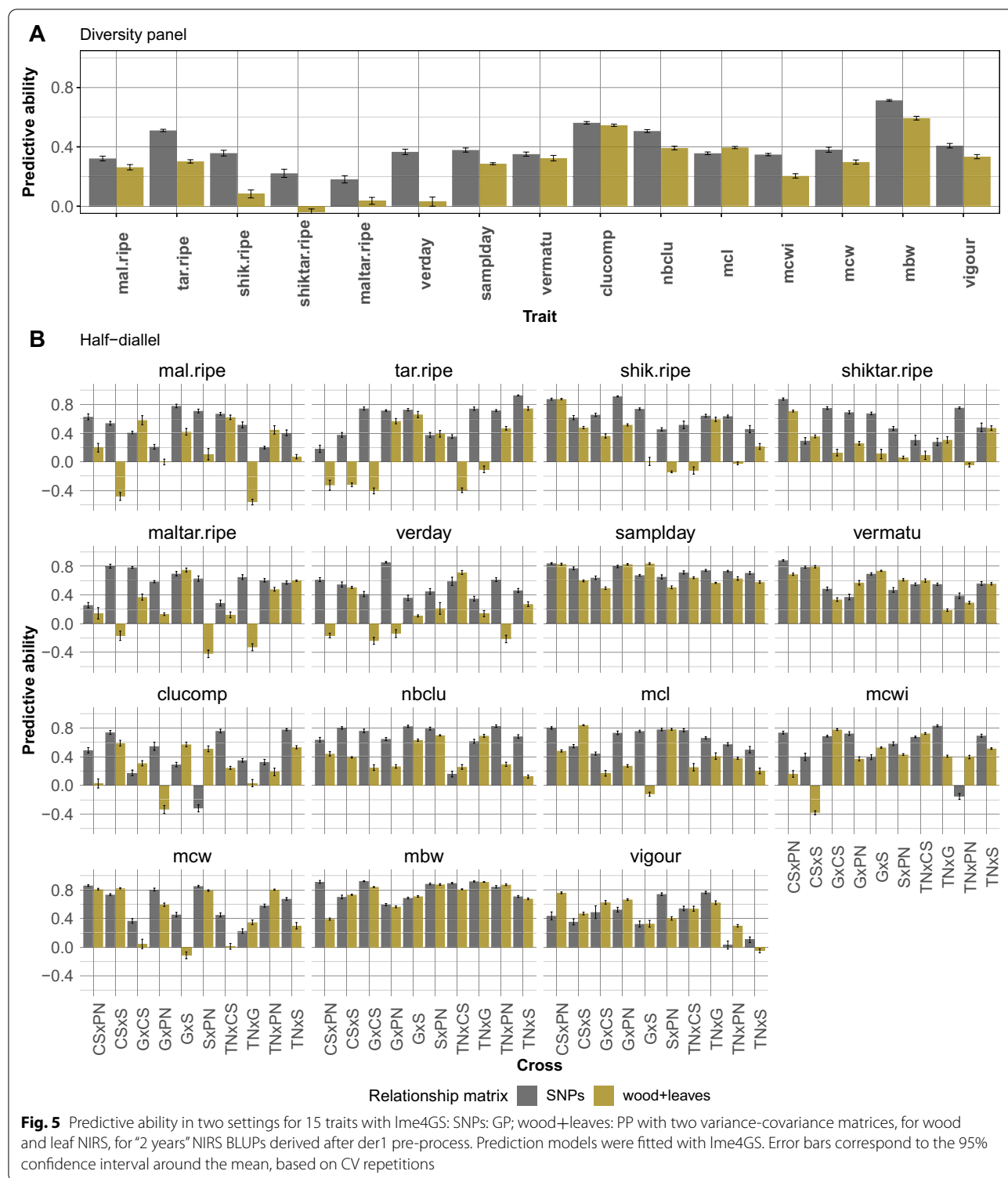
We observed higher variance in PA in the half-diallel than in the diversity panel, because in the half-diallel, PA distribution was over 10 crosses in addition to the 6 years × tissues model combinations retained (see above). Average PA for the best method was slightly higher in the half-diallel (0.31) than in the diversity panel (0.26).

We compared PA for all pre-processes, after selecting the best method for each population (Additional file 1: Fig. S4). We found that **der1** and **der2** pre-processes gave close results, with a slight superiority of **der1** overall. Therefore, we kept only this pre-process in subsequent analyses.

Phenomic prediction using NIRS collected over one or two years and tissues

We further compared PP models including a single vs. both NIRS BLUP matrices obtained from wood and leaves. For each tissue configuration, we used the NIRS BLUPs derived from the above-described year configurations (2020, 2021 or both). For single tissue configurations, we used the best method selected above in each population, and one NIRS BLUP matrix was fitted. For





the wood+leaves configuration in both populations, two NIRS BLUP matrices (one for wood and one for leaves) were fitted using lme4GS package.

For both populations, the nine configurations tested resulted in close PA distributions (Fig. 4). Yet, “2 years” and “wood+leaves” configurations overall gave the best average PA values. We thus retained only multi-year and

multi-tissue PP results for subsequent comparison with GP.

Finally, PA was slightly higher in the half-diallel on average, with a larger variance originating from differences between crosses (see hereafter).

If we now turn to details per trait, the results show that, within the diversity panel, each trait displayed nearly the same PA for the different tissue configurations, for PA values above 0.2 (Additional file 1: Fig. S5). In the half-diallel, there were larger differences between tissue configurations. However, this factor still had far less impact on PA than cross or trait.

Overall average PA of PP for “2 years” and “wood+leaves” configuration was 0.27 in the diversity panel and 0.35 in the half-diallel (Fig. 4). PA values per trait ranged from -0.04 for **shiktar.ripe** to 0.59 for **mbw** in the diversity panel (Additional file 1: Fig. S5A), and from 0.09 for **mal.ripe** to 0.72 for **mbw** in the half-diallel (note that in the half diallel, PA values per trait are averaged over the 10 crosses). However, large differences in PA of PP were observed within a trait at the cross level in the half-diallel for “2 years” and “wood+leaves” configuration, such as for **tar.ripe**, from -0.49 for GxCS to 0.74 for TNxS (Fig. 5B and Additional file 1: Fig. S5B). Comparatively, differences at the cross level were lower for GP (Additional file 1: Fig. S6). The best predicted cross with PP over all traits was GxS (average PA of 0.41) and the worst one was TNxG (0.29) (Additional file 1: Fig. S7). For some crosses and traits, PA values could be above 0.8, the maximum PA for PP being 0.91 for **mbw** and TNxG (Additional file 1: Fig. S5B).

Comparison of PP with GP

Before comparing PP with GP, we applied GP on both populations with the two methods previously compared for PP (Additional file 1: Fig. S6). We found that lme4GS was overall the best method in both populations, hence we retained this method for the following comparison. Like this was the case for PP, differences between methods appeared to be more pronounced in the half-diallel than in the diversity panel.

The PA reached by PP was generally lower to that of GP in both populations. Differences between PP and GP was small for a few traits and for some half-diallel crosses (**samplday**, **vermatu** and **mbw**) (Fig. 5). PP even in some cases outperformed GP in the half-diallel, such as for CSxPN, GxCS, GxPN and **vigour**, or GxCS, SxPN, TNxPN and **clucomp**. Differences in PA between PP and GP were lower in the diversity panel than in the half-diallel.

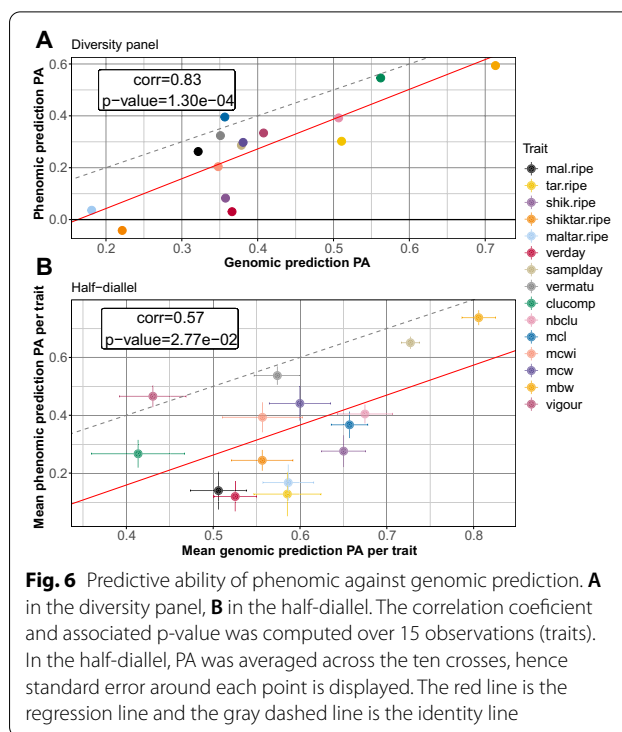


Fig. 6 Predictive ability of phenomic against genomic prediction. **A** in the diversity panel, **B** in the half-diallel. The correlation coefficient and associated p-value was computed over 15 observations (traits). In the half-diallel, PA was averaged across the ten crosses, hence standard error around each point is displayed. The red line is the regression line and the gray dashed line is the identity line

In the diversity panel, PA of PP was significantly higher (non-overlapping error bar) than PA of GP for one trait (**mcl**) and non-significantly different for two other traits (**clucomp** and **vermatu**) (Fig. 5A). In the half-diallel, PA of PP was significantly higher than PA of GP for 28 trait × cross combinations out of 150, while this difference was not significant in 17 other cases (Fig. 5B). In all other cases, PA of PP was lower than PA of GP.

In Fig. 6, we further compared mean PAs of PP and GP per trait in each population. In both populations, the slope of the regression model was close to 1 and the intercept to -0.2. This suggests that PA of PP and GP follow the same ranking, independently of the trait. However, this regression had a much lower R^2 in the half-diallel than in the diversity panel.

Enhancing genomic prediction using NIRS

Another possible way of using NIRS is to add it into the predictive model together with SNPs, in order to increase PA. We thus implemented multi-BLUP models with SNPs and NIRS BLUPs and compared them to GP models in each population.

Overall, for both populations and for all traits, differences in PA between SNP based model and different combined GP+PP models were small (Additional file 1: Fig. S8). In the diversity panel, combining wood NIRS

with SNPs led to the best PA (0.405), closely followed by leaves NIRS + SNPs (0.403), wood NIRS + leaves NIRS + SNPs (0.402) and SNPs alone (0.400). In the half-diallel, SNPs alone gave the highest PA (0.595), followed by wood NIRS + leaves NIRS + SNPs (0.587), leaves NIRS + SNPs (0.576), and wood NIRS + SNPs (0.569).

Nevertheless, adding NIRS to a predictive model could lead to minor (non-significant) improvements in PA for some traits, compared to classic GP. Combining GP + PP from wood NIRS slightly increased PA over the GP model for two traits in the diversity panel (**clucomp** and **mcl**) (Additional file 1: Fig. S8A). In the half-diallel, the difference in average PA with GP was much more variable among traits, with an increase for **vigour**, **clucomp**, **vermatu** and **samplday**, and a decrease for **mal.ripe**, **tar.ripe**, **shik.ripe**, **shiktar.ripe**, **maltar.ripe**, **nbclu**, **mcl** and **mcwi** (Additional file 1: Fig. S8B).

Discussion

So far, PP has only been implemented in a reduced number of species and traits. This study provides the first use of PP in grapevine, within two complementary populations: a diversity panel and a half-diallel. Besides, we tested PP for 15 traits, belonging to four categories: berry composition, phenology, morphological traits and vigour. We first showed that NIRS variability was partly of genotypic origin. We then tested several parameters for PP implementation. We found that pre-processing had a little impact on NIRS heritability and PA. Nevertheless, using genotypic values from NIRS resulted in a strong increase in PA, while tissues and years tested had a relative small impact on PA. Finally, we found that PP could yield PA values close to or even higher than GP ones, for some traits and crosses.

NIRS variance components and co-inertia with SNPs

Genotype and derived interaction variables had a fairly moderate impact on total variance observed between spectra (Fig. 1). The genotypic effect was best captured in single-tissue analyses. This was not surprising, because the genetic signal at a given wavelength relies on molecules specific to each tissue. Then, mixing both tissues into a single model led to no overall genetic effect and to strong *geno:tissue* interaction. This tendency was also observed, to a smaller extent, in the multi-year analyses. This also suggests that different tissues bring non redundant genetic information. This was confirmed by co-inertia analysis, which evidenced that NIRS matrices from wood and leaves were more correlated to the SNP matrix than to each other.

Interestingly, co-inertia analysis showed that multi-year NIRS BLUP matrices were slightly more correlated with the genomic relationship matrix than single-year ones,

despite lower genotypic variance. This implies that the genotypic part of NIRS estimated by multi-year analysis could be more related to the genetic signal. Thus, genetic signal ignoring genotype-by-environment interactions could be better captured when several years are combined, this was also the case in Galán et al. [13] for which multi-year spectra resulted in higher PA values.

Comparatively to genotype-related effects, among non-residual variance components, x effect displayed a large variance along wavelengths (Fig. 1). This effect actually corresponds to a row effect and might be due to the experimental design, which encompasses field effects and spectra collection design, both being confounded. Indeed, leaf discs and wood shoots were both sampled and scanned row by row, sometimes several weeks apart for NIRS collection. However, we cannot determine whether this x effect comes from the tissue sampling, i.e., sampling time (over a day), soil heterogeneity; or from the NIRS measurement step, i.e., device calibration, differential storage time, air humidity. Our results underline the importance of accounting such experimental effects in order to improve the genetic signal captured and thus prediction. In further experiments, one could increase the number of spectra per plot and randomize NIRS measurements, in order to determine if the x effect observed here was due to measurement or sampling and to reduce it. Other studies that fitted a linear model for each wavelength did not introduce field coordinates as effects (e.g. [12, 15, 16]). But the first and last studies were based on hyperspectral images taken with aircraft flights, that is with an experimental design less prone to plot location effect, and the second study fitted a linear model with only block and environmental effects.

Galán et al. [12] found a mean heritability value of 0.73 for wavelength reflectances, which is substantially higher than the values we observed (Additional file 1: Fig. S1). However, we did not use the same heritability formula. Montesinos-López et al. [20] also reported overall higher heritability values ranging from 0.6 to 0.8 for most time points, with strong variations depending on the environment (water availability) and time-point.

We found higher heritability and genetic variance in the diversity panel than in the half-diallel. Yet, PA were generally higher in the half-diallel. In Rincent et al. [24], genetic variance estimates per wavelength between wheat and poplar were consistent with PA in these species, i.e., they evidenced higher PA values in wheat than in poplar. On the opposite, our results on co-inertia analysis were consistent with PA values: correlation between SNP and NIRS BLUPs matrices was higher in the half-diallel than in the diversity panel (Fig. 2). This suggests that co-inertia analysis is more relevant to compare configurations

for NIRS BLUP than variance components. The higher co-inertia observed between SNP and NIRS BLUP in the diallel with respect to the diversity panel is likely to be explained by the higher genetic structure in the half-diallel, or because the half-diallel is in better health than the diversity panel, which is older and overgrafted. Actually, it was surprising that NIRS could capture genetic structure, i.e., in our case the *subpopulation* effect in the diversity panel and the *cross* effect in the half-diallel. Although variance components for *subpopulation* and *cross* remained moderate (Fig. 1), adding the corresponding BLUP effects to genotypic effects led to a sharp increase in correlation between NIRS and SNP matrices (Additional file 1: Fig. S2). Further in-depth studies are required to better understand whether this observation could be specific to some subpopulations or families.

Optimizing PP

Among the parameters tested, some had substantial impact on PA, while others had only negligible impact. Namely, using NIRS via BLUP analysis instead of merely average spectra per genotype led to a strong increase in PA (Fig. 3). This was probably associated with the strong x effect we observed in variance analysis. Such a difference had never been reported before, as studies obtained PP results either from *base* (such as [6, 24]) or BLUE (such as [15, 16]) spectra, without comparing both configurations.

Surprisingly, the prediction method also had notable impact on PA: using rrBLUP or GBLUP models gave different PA in the half-diallel, while differences in PA between methods were lower in the diversity panel (Fig. 3). Yet, GBLUP and rrBLUP models are expected to perform similarly when the regularization parameter in ridge regression is equal to σ_e^2/σ_g^2 [14]. In our analysis, this parameter value was chosen by cross-validation using cv.glmnet function. The higher relatedness between genotypes within the half-diallel than within the diversity panel (Brault et al. [4], Fig. 1a) may boost GBLUP models compared to rrBLUP in this population. In future investigations, one could use variable selection method such as LASSO to select the most relevant wavelengths for computing the relationship matrix from NIRS BLUP. Such variable selection was performed by Galán et al. [12] and resulted in higher PA.

On the opposite, using single-year, single tissue, multi-year, or multi-tissue NIRS BLUPs and all pre-processes except **smooth** gave very similar results over all traits and crosses (Fig. 4), with a slight superiority of multi-year model overall. This was consistent with the results of co-inertia analysis (Additional file 1: Fig. S3). In Rincent et al. [24], the multi-tissue analysis for wheat with leaf and grain combined gave similar PA as for single-tissue analysis. As the combination

of two tissues for PP was only done in one other study [24], further work needs to be done to assess these conclusions.

For a given trait, both tissues tested gave similar PA for the diversity panel (Additional file 1: Fig. S5A). For the half-diallel, more differences were observed between tissues, and much larger differences were observed between crosses (Additional file 1: Fig. S5B). However, no cross was consistently well or poorly predicted for all traits, suggesting a strong cross \times trait interaction. These large disparities among crosses were consistent with the GP results obtained in the same population by Brault et al. [4].

Comparison between PP and GP

PP is supposed to better account for $G \times E$ than GP. However, it was shown in Rincent et al. [24] that PP could still reach good PA values when NIRS for TS were taken in an environment different from the one in which VS was phenotyped, i.e., when accounting for $G \times E$ was not possible. In this study, we could not assess whether PP accuracy partly relied on location-related $G \times E$, because phenotypes and NIRS came from a single location. Nevertheless, phenotypes were measured in 2011-2012 and 2013-2017 in the diversity panel and half-diallel populations, respectively, whereas NIRS were measured in 2020-2021 in both populations. Vintage (year) effect is also part of $G \times E$ and it is likely that 2020 or 2021 could display some differences in terms of weather with phenotyping years. For training and validation model, we used genotypic BLUPs of both phenotypic data, thereby removing *year* and *geno:year* effects. We found that PA seemed not to be impacted by NIRS year for all traits studied, suggesting that vintage has a negligible effect on PA when genotypic BLUPs are used.

We found that PP could compete with GP for some traits in both populations, despite moderate genetic variance estimated from NIRS. However, the number of traits for which PP outperformed GP remained low. These results were close to those of Rincent et al. [24] on poplar. In our case, one explanation could be that NIRS came from tissues sampled in 2020 and 2021, while phenotypes were measured in 2011-2012 and 2013-2017 in the diversity panel and half-diallel, respectively. Thus, we couldn't take into account for $G \times E$ from vintage effect. As a perspective, it would be interesting to compare PA when spectra are measured the same year as phenotyping or not. In such case, one could explicitly model vintage effects in spectra to further increase PA.

Implementation of PP in perennial breeding programs

What we tested (spectra and phenotypes collected several years apart) is a novelty compared to existing studies

in phenomic prediction. Indeed, spectra are usually collected the same years as phenotypes. Hence, phenomic prediction is relying both on genetics and $G \times E$ interactions. We intentionally excluded $G \times E$ interactions and maximized the genetic signal in spectra. Thus, we did not expect that PP could outperform GP, as the genetic signal in spectra is most likely less precise than genotyping. We measured the predictive ability of phenomic prediction, that relies only on genetics. Such measure is crucial for the implementation of phenomic prediction in breeding program, especially in perennial species, since we expect to predict genotypic values several years before phenotyping. A further step would be to confirm that spectra from seedlings and mature plants provide the same amount of genetic information.

Nevertheless, even when PP does not outperform GP, it may still be interesting in breeding, because of its lower cost and increased throughput compared to genotyping. Moreover, when a trait was well-predicted with GP, we found that it was also well-predicted with PP, with a global shift of -0.2 in PA (Fig. 6). This suggests that PP PA truly relies on genetic variability and that PP could be applied indifferently for all traits. Even though this study is the first one implementing PP on so many traits (15), these conclusions remain to be confirmed on other species and traits. Based on a simulated breeding program from Rincent et al. [24] and on the relative GP and PP reliability that we observed, we are still expecting a positive genetic gain by switching from GP to PP, under a constant breeding program budget.

We implemented that setting, in order to test whether combining NIRS and SNP could increase PA compared to GP, by taking other genetic effects into account. However, as we used NIRS BLUPs, we only maximized the genetic variance part of spectra, we thus intentionally excluded $G \times E$. Therefore, the fact that adding NIRS to GP model did not result in any increase in PA is consistent with our spectra processing. Cuevas et al. [6] and Galán et al. [12] found slight to noticeable improvement in PA when NIRS was added to the model, compared to GP model with SNPs only; difference in PA was at most 0.01 in Cuevas et al. [6] and up to 0.1 in Galán et al. [12]. Both studies are however so different than ours that it is difficult to explain these different behaviors.

As a conclusion, we provided the first implementation of PP in grapevine. The number of traits studied allowed us to put forward a correlation between PA of GP and PP, suggesting that PP relies on a genetic basis. Such a correlation was never reported before. We expect that the shift of PA between PP and GP of -0.2 would be reduced if year of phenotyping and spectra measurement are the same. Still, PP has shown its interest for breeding over a wide range of traits.

Supplementary Information

The online version contains supplementary material available at <https://doi.org/10.1186/s13007-022-00940-9>.

Additional file 1: Figure S1. Heritability distribution across wavelengths for each pre-process. **Figure S2.** Co-inertia analysis between SNP and multi-year wood and leaves NIRS matrices. **Figure S3.** Co-inertia analysis between SNP, single and multi-year wood and leaves NIRS matrices. **Figure S4.** Distribution of phenomic prediction predictive ability per pre-process and per trait. **Figure S5.** Predictive ability of phenomic prediction with a single vs both tissues. **Figure S6.** Comparison of methods for genomic prediction. **Figure S7.** Distribution of phenomic prediction predictive ability over 15 traits in each half-diallel cross. **Figure S8.** Predictive ability of combined vs genomic prediction models.

Acknowledgements

This work has been realized with MESO@LR-Platform at the University of Montpellier.

Author contributions

VS, AD, PT and LLC conceived the idea of the study and contributed to funding acquisition; TP, PF and AD obtained the phenotypic data used in this work; YB, GB, MT, JL and CB measured spectra; ME and PR gave advices on spectrometer use; CB and JL performed and interpreted results; AD conceived the half-diallel population; PT is the PhD supervisor of CB; CB wrote the original draft, which was reviewed and edited by all authors. All authors read and approved the final manuscript.

Funding

Partial funding of CB's PhD was provided by ANRT (Grant Number 2018/0577), IFV and Inter-Rhône. Spectra collection was partially supported by the project OASis funded the French ministry of Agriculture and Food (CASDAR, C 2020-5). The preparation of this manuscript was partly supported by the project Sel-GenVit funded by the French National Research Agency (ANR-19-ECOM-0006).

Availability of data and materials

All analyses were conducted using free and open-source software, mostly R. Genotypic values and genotypic data for half-diallel and diversity panel populations are available at <https://doi.org/10.15454/PNQUQU>. Spectra, R scripts and result tables have been deposited in the INRAE data portal: <https://doi.org/10.15454/BICRFX>.

Declarations

Ethics approval and consent to participate

The authors declare that the experiments comply with the current laws of the country in which they were carried out.

Competing interests

The authors declare that they have no conflict of interest.

Author details

¹UMR AGAP Institut, Univ Montpellier, CIRAD, INRAE, Institut Agro Montpellier, Montpellier 34398, France. ²UMT Geno-Vigne®, IFV, INRAE, Institut Agro Montpellier, 34398 Montpellier, France. ³Institut Français de la vigne et du vin, 34398 Montpellier, France.

Received: 21 April 2022 Accepted: 24 July 2022

Published online: 05 September 2022

References

- Barnes RJ, Dhanoa MS, Lister SJ. Standard normal variate transformation and de-trending of near-infrared diffuse reflectance spectra. *Appl Spectrosc.* 1989;43(5):772–7.

2. Bernardo R. Prediction of maize single-cross performance using RFLPS and information from related hybrids. *Crop Sci.* 1994. <https://doi.org/10.2135/cropsci1994.0011183X003400010003x>.
3. Brault C, Doligez A, Cunff L, Coupel-Ledru A, Simonneau T, Chiquet J, This P, Flutre T. Harnessing multivariate, penalized regression methods for genomic prediction and QTL detection of drought-related traits in grapevine. *G3.* 2021. <https://doi.org/10.1093/g3journal/jkab248>.
4. Brault C, Segura V, This P, Le Cunff L, Flutre T, François P, Pons T, Péros JP, Doligez A. Across-population genomic prediction in grapevine opens up promising prospects for breeding. *Horticulture Research.* 2022. <https://doi.org/10.1093/hr/uhac04>.
5. Caamal-Pat D, Pérez-Rodríguez P, Crossa J, Velasco-Cruz C, Pérez-Elizalde S, Vázquez-Peña M. lme4GS: an R-package for genomic selection. *Front Genet.* 2021. <https://doi.org/10.3389/fgene.2021.680569>.
6. Cuevas J, Montesinos-López O, Juliana P, Guzmán C, Pérez-Rodríguez P, González-Bucio J, Burguenio J, Montesinos-López A, Crossa J. Deep kernel for genomic and near infrared predictions in multi-environment breeding trials. *G3.* 2019;9(9):2913–24. <https://doi.org/10.1534/g3.119.400493>.
7. Dolédec S, Chessel D. Co-inertia analysis: an alternative method for studying species: environment relationships. *Freshw Biol.* 1994;31(3):277–93.
8. Elshire RJ, Glaubitz JC, Sun Q, Poland JA, Kawamoto K, Buckler ES, Mitchell SE. A robust simple genotyping-by-sequencing (GBS) approach for high diversity species. *PLOS ONE.* 2011. <https://doi.org/10.1371/journal.pone.0019379>.
9. Flutre T, Le Cunff L, Fodor A, Launay A, Romieu C, Berger G, Bertrand Y, Beccavin I, Bouckennooghe V, Roques M, Pinasseau L, Verbaere A, Sommerer N, Cheynier V, Bacilieri R, Boursiquot JM, Lacombe T, Laucou V, This P, Péros JP, Doligez A. Genome-wide association and prediction studies using a grapevine diversity panel give insights into the genetic architecture of several traits of interest. *G3.* 2022. <https://doi.org/10.1093/g3journal/jkac103>.
10. Fodor A, Segura V, Denis M, Neuenschwander S, Fournier-Level A, Chatelet P, Homa FAA, Lacombe T, This P, Le Cunff L. Genome-wide prediction methods in highly diverse and heterozygous species: proof-of-concept through simulation in grapevine. *PLoS ONE.* 2014. <https://doi.org/10.1371/journal.pone.0110436>.
11. Friedman J, Hastie T, Tibshirani R. Regularization paths for generalized linear models via coordinate descent. *J Stat Softw.* 2010. <https://doi.org/10.18637/jss.v033.i01>
12. Galán RJ, Bernal-Vasquez AM, Jebsen C, Piepho HP, Thorwarth P, Steffan P, Gordillo A, Miedaner T. Integration of genotypic, hyperspectral, and phenotypic data to improve biomass yield prediction in hybrid rye. *Theor Appl Genet.* 2020. <https://doi.org/10.1007/s00122-020-03651-8>.
13. Galán RJ, Bernal-Vasquez AM, Jebsen C, Piepho HP, Thorwarth P, Steffan P, Gordillo A, Miedaner T. Early prediction of biomass in hybrid rye based on hyperspectral data surpasses genomic predictability in less-related breeding material. *Theor Appl Genet.* 2021;134(5):1409–22. <https://doi.org/10.1007/s00122-021-03779-1>.
14. Habier D, Fernando RL, Dekkers JCM. The impact of genetic relationship information on genome-assisted breeding values. *Genetics.* 2007;177(4):2389–97. <https://doi.org/10.1534/genetics.107.081190>.
15. Krause MR, González-Pérez L, Crossa J, Pérez-Rodríguez P, Montesinos-López O, Singh RP, Dreisigacker S, Poland J, Rutkoski J, Sorrells M, Gore MA, Mondal S. Hyperspectral reflectance-derived relationship matrices for genomic prediction of grain yield in wheat. *G3.* 2019. <https://doi.org/10.1534/g3.118.200856>.
16. Lane HM, Murray SC, Montesinos-López OA, Montesinos-López A, Crossa J, Rooney DK, Barrero-Farfan ID, Fuente GNDL, Morgan CLS. Phenomic selection and prediction of maize grain yield from near-infrared reflectance spectroscopy of kernels. *Plant Phenome J.* 2020. <https://doi.org/10.1002/ppj2.20002>.
17. Meng C, Kuster B, Culhane AC, Gholami AM. A multivariate approach to the integration of multi-omics datasets. *BMC Bioinform.* 2014;15(1):162. <https://doi.org/10.1186/1471-2105-15-162>.
18. Meuwissen T, Hayes B, Goddard M. Prediction of total genetic value using genome-wide dense marker maps. *Genetics.* 2001. <https://doi.org/10.1093/genetics/157.4.1819>.
19. Min EJ, Safo SE, Long Q. Penalized co-inertia analysis with applications to -omics data. *Bioinformatics.* 2019;35(6):1018–25. <https://doi.org/10.1093/bioinformatics/bty726>.
20. Montesinos-López OA, Montesinos-López A, Crossa J. Predicting grain yield using canopy hyperspectral reflectance in wheat breeding data. *Plant Methods.* 2017;13(1):4. <https://doi.org/10.1186/s13007-016-0154-2>.
21. Morales-Castilla I, García de Cortázar-Atauri I, Cook BI, Lacombe T, Parker AK, van Leeuwen C, Nicholas KA, Wolkovich EM. Diversity buffers winegrowing regions from climate change losses. *Proc Natl Acad Sci.* 2020;117(6):2864–9. <https://doi.org/10.1073/pnas.1906731117>.
22. Nicolas SD, Péros JP, Lacombe T, Launay A, Le Paslier MC, Bérard A, Mangin B, Valière S, Martins F, Le Cunff L, Laucou V, Bacilieri R, Dereeper A, Chatelet P, This P, Doligez A. Genetic diversity, linkage disequilibrium and power of a large grapevine (*Vitis vinifera* L) diversity panel newly designed for association studies. *BMC Plant Biol.* 2016;16(1):74. <https://doi.org/10.1186/s12870-016-0754-z>.
23. Piepho HP, Möhring J. Computing heritability and selection response from unbalanced plant breeding trials. *Genetics.* 2007;177(3):1881–8. <https://doi.org/10.1534/genetics.107.074229>.
24. Rincet R, Charpentier JP, Fèvre-Rampant P, Paux E, Le Gouis J, Bastien C, Segura V. Phenomic selection is a low-cost and high-throughput method based on indirect predictions: proof of concept on wheat and poplar. *G3.* 2018. <https://doi.org/10.1534/g3.118.200760>.
25. Robert P, Escoufier Y. A unifying tool for linear multivariate statistical methods: the RV-coefficient. *J R Stat Soc Ser C Appl Stat.* 1976;25(3):257–65. <https://doi.org/10.2307/2347233>.
26. Robert P, Auzanneau J, Goudemand E, Oury FX, Rolland B, Heumez E, Bouchet S, Le Gouis J, Rincet R. Phenomic selection in wheat breeding: Identification and optimisation of factors influencing prediction accuracy and comparison to genomic selection. *Theor Appl Genet.* 2022. <https://doi.org/10.1007/s00122-021-04005-8>.
27. Savitzky A, Golay MJE. Smoothing and differentiation of data by simplified least squares procedures. *Anal Chem.* 1964;36:1627–39.
28. Schrag TA, Westhues M, Schipprack W, Seifert F, Thiemann A, Scholten S, Melchinger AE. Beyond genomic prediction: combining different types of omics data can improve prediction of hybrid performance in maize. *Genetics.* 2018;208(4):1373–85. <https://doi.org/10.1534/genetics.117.300374>.
29. Tello J, Roux C, Chouiki H, Laucou V, Sarah G, Weber A, Santoni S, Flutre T, Pons T, This P, Péros JP, Doligez A. A novel high-density grapevine (*Vitis vinifera* L.) integrated linkage map using GBS in a half-diallel population. *Theor Appl Genet.* 2019;132(8):2237–52. <https://doi.org/10.1007/s00122-019-03351-y>.

Publisher's Note

Springer Nature remains neutral with regard to jurisdictional claims in published maps and institutional affiliations.

Ready to submit your research? Choose BMC and benefit from:

- fast, convenient online submission
- thorough peer review by experienced researchers in your field
- rapid publication on acceptance
- support for research data, including large and complex data types
- gold Open Access which fosters wider collaboration and increased citations
- maximum visibility for your research: over 100M website views per year

At BMC, research is always in progress.

Learn more biomedcentral.com/submissions

